CHEMISTRY
A European Journal

A Journal of
ChemPubSoc Europe

Accepted Article

Title: Development of lysosome-targeted fluorescent probes for Cys by regulating BODIPY molecular structure

Authors: Jinhua Gao, Yuanfang Tao, Jian Zhang, Nannan Wang, Xin Ji, Jinling He, Yubing Si, and Weili Zhao

To be cited as: *Chem. Eur. J.* 10.1002/chem.201902301

Link to VoR: http://dx.doi.org/10.1002/chem.201902301

Supported by
ACES

WILEY-VCH

10.1002/chem.201902301

WILEY-VCH

Development of lysosome-targeted fluorescent probes for Cys by regulating BODIPY molecular structure

Jinhua Gao,[a] Yuanfang Tao,[a] Jian Zhang,*[a] Nannan Wang,[a] Xin Ji,[a] Jinling He,[a] Yubing Si,*[c] and Weili Zhao*[ab]

Abstract: Our early discovery suggested that substituents on 1,7 positions delicately modulate the sensing ability of the *meso*-arylmercapto BODIPY to biothiols. In this work, we continue to investigate the impact of delicate modulations on the sensing ability. Therefore, we designed and developed 1,7-dimethyl, 3,5-diaryl substituted BODIPY and its conformationally restricted species with *meso*-arylmercapto moiety (**DM-BDP-SAr** and **DM-BDP-R-SAr**) as selective fluorescent probes for Cys. Moreover, the lysosome-target probes (**Lyso-S** and **Lyso-D**) based on **DM-BDP-SAr** carrying one or two morpholinoethoxy moieties were developed. They were able to detect Cys selectively *in vitro* with low detection limits. Both **Lyso-S** and **Lyso-D** localized nicely in lysosomes in living HeLa cells and exhibited red fluorescence for Cys. Moreover, a novel fluorescence quenching mechanism was proposed from the calculations by density functional theory (DFT). The probes may go through intersystem crossing (from singlet excited state to triplet excited state) to result in fluorescence quenching.

Introduction

As important biomolecules, biothiols such as cysteine (Cys), homocysteine (Hcy) and glutathione (GSH) play vital roles in a wide range of physiological and pathological processes arising from their biological redox chemistry.[1,2] Cys and Hcy are essential biological molecules required for detoxifying function, immunological competence, as well as growth and delay of ageing of cells and tissues in living systems.[3] Meanwhile, GSH is the most abundant intracellular non-protein thiol (1–10 mM) and a biomarker of oxidative stress.[4,5] It has been revealed that GSH plays a critical role in controlling oxidative stress in order to maintain the redox homeostasis for cell growth and function.[6] Aberrant levels of biothiols in humans may contribute to various diseases. In addition, biothiols are closely associated with proteolysis in the lysosome which reduces disulphide bonds.[7,8] It is believed that GSH is involved in the stabilization of lysosome's membranes, whereas Cys is an effective stimulator of albumin degradation in liver lysosomes.[9-11] Therefore, selective determination of biothiols is of great importance for various investigations in biochemistry as well as assistance in diagnosis of the related diseases in clinic.

A large number of innovative fluorescent probes have been discovered to distinguish and measure biothiols.[12-31] Some impressive works have succeeded in differentiating GSH from Cys and Hcy.[19-27] However, it is still a challenge to construct probes for discriminating Cys from Hcy due to the similar pKa and steric congestion of Cys and Hcy, which also frequently suffers from drawbacks such as unsatisfied selectivity, long response time, and undesired spectra overlap.[22,32-40] We are devoted to designing and developing new fluorescent probes capable of effective differentiation of Cys, Hcy, GSH, and favourably with lysosome targeting capability.

Our group has considerable interest in the design and synthesis of BODIPY-based dyes as fluorescent probes for various biothiols species.[41-49] The early works relying on the *meso* substitution strategy of BODIPY were exhibited in Scheme 1. With no substitution at 1,7 positions of BODIPY skeleton (**BDP-SAr**), differentiate Cys/Hcy from GSH in dual emission channel mode was realized (Scheme 1a).[43] On the other hand, when 1,7-dimethyl groups present on BODIPY skeleton (**TM-BDP-SAr**), we found that differentiation in dual channel mode was changed to Cys from Hcy/GSH (Scheme 1b).[47] In addition, we also reported 1,7-diaryl substituted BODIPY and its conformationally restricted species (**DPh-BDP-R-SAr**) for highly selective detection of Cys and Hcy rather than bulky GSH (Scheme 1c).[48] The steric congestion of the 1,7-diphenyl groups completely blocked nucleophilic attack from bulky GSH. These results implied the important functions of the steric congestion at the 1,7 positions of BODIPY for the selective biothiols recognition.

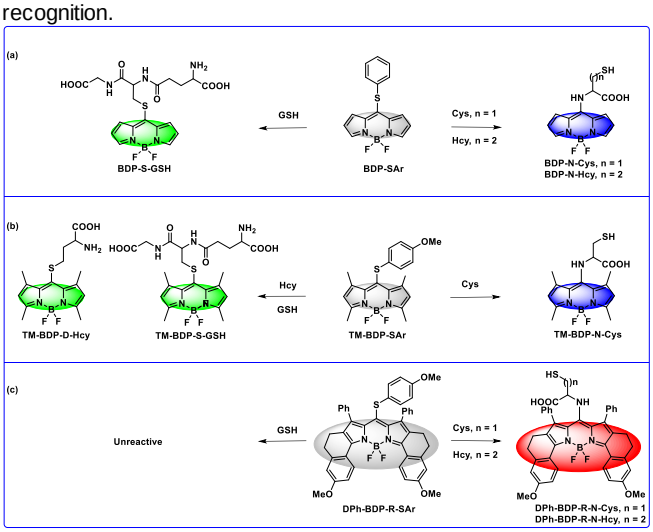

Scheme 1. Reaction mechanisms of BODIPY-based probes with biothiols in our group's previous studies.

[a] J. Gao, Y. Tao, N. Wang, X. Ji, Dr. J. He, Dr. J. Zhang*, Prof. W. Zhao*
Key Laboratory for Special Functional Materials of Ministry of Education, School of Materials Science and Engineering, Henan University
Kaifeng 475004, P. R. China.
E-mail: zhangjian861208@126.com; zhaow@henu.edu.cn
[b] Prof. W. Zhao*
School of Pharmacy, Institutes of Integrative Medicine, Fudan University,
Shanghai, 201203, P. R. China.
[c] Prof. Y. Si*
Henan Key Laboratory of Nanocomposites and Applications, Institute of Nanostructured Functional Materials, Huanghe Science and Technology College, Zhengzhou 450006, P. R. China
Supporting information for this article is given via a link at the end of the document.

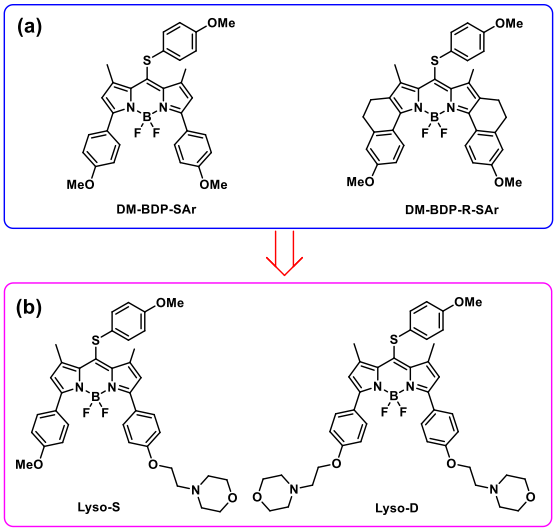

Scheme 2. Chemical structures of the probes designed.

We were curious to know whether 1,7-dimethyl substitution which enabled biothiols detection and differentiation of Cys from Hcy/GSH in dual emission channel in blue-green region could be extended to more favorable green-red region, and whether structure conformation restriction will affect the recognition. Moreover, we were also interested in developing lysosome-targeted version. Hence, we designed and synthesized 1,7-dimethyl, 3,5-diaryl substituted BODIPY and its conformationally restricted species carrying a p-methoxyphenylmercapto moiety at *meso* position (**DM-BDP-SAr** and **DM-BDP-R-SAr**, Scheme 2a). Moreover, the lysosome targeted probes (**Lyso-S** and **Lyso-D**) were designed by attaching a single or dual morpholinoethoxy group onto the phenyl moiety (Scheme 2b). The Hela cells were popularly used for cell fluorescence imaging due to the rapidly growing and reproduction, so we chose HeLa cells to identify the performence of **Lyso-S** and **Lyso-D**.

Results and Discussion

Syntheses of probes

The designed probes were prepared using the synthetic route as shown in Scheme 3.

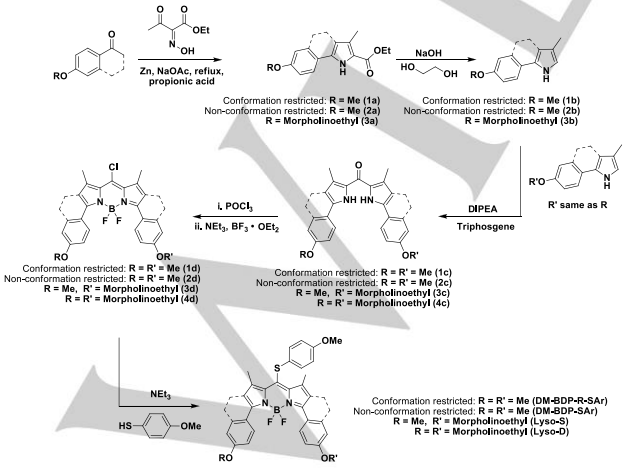

Scheme 3. Synthesis of probes.

The required pyrrole skeleton (**1a**-**3a**) can be constructed using Knorr pyrrole synthesis starting from 6-methoxy tetralone or from 3-acetyl benzene derivative with *para* methoxy or morpholinoethoxy substitutent. Hydrolysis and decarboxylation under alkaline conditions afforded the desired pyrroles (**1b**-**3b**). Treatment of the pyrrole with triphosgene in the presence of diisopropylethylamine and addition another portion of pyrrole provided the dipyrrylmethanone (**1c**-**4c**). After reacting with $POCl_3$ to *meso* chloro dipyrromethene and complexation with boron trifluoride etherate in the presence of base, the desired BODIPY dyes (**1d**-**4d**) were obtained. Using 4-methoxythiophenol to replace the chloro group with the assistance of mild base resulted in the desired probes (**DM-BDP-SAr**, **DM-BDP-R-SAr**, **Lyso-S**, and **Lyso-D**).

Spectroscopic properties of DM-BDP-SAr and DM-BDP-R-SAr and the responses to biothiols

DM-BDP-SAr possessed absorption maximum at 591 nm, which was shorter than that of **DM-BDP-R-SAr** (670 nm) in acetonitrile/PBS buffer (1 : 1, v/v, 10 mM, pH 7.4) and low fluorescence at 37 °C was noticed (Figure 1). In the presence of Cys, drastic changes in the absorption (with absorption at 470 nm) and fluorescence (enhanced emission at 562 nm) were observed in 15 min for **DM-BDP-SAr** (Figures 1a and 1b). The absorption spectra varied in a ratiometric response with an isosbestic point at 506 nm, which could be adopted for the quantitative estimation the concentration of Cys. In stark contrast, when Hcy was reacted with **DM-BDP-SAr**, only very minor changes were found both in the absorption and emission spectra (Figure S1). Moreover, GSH was also investigated and very slow reaction rate was identified (Figure S1). Keep in mind that our initial design purpose was trying to develop dual emission channel mode probe(s) in the green-red region, herein unexpected selective detection of Cys was achieved. More astonishingly, the Stokes' shift of 100 nm was

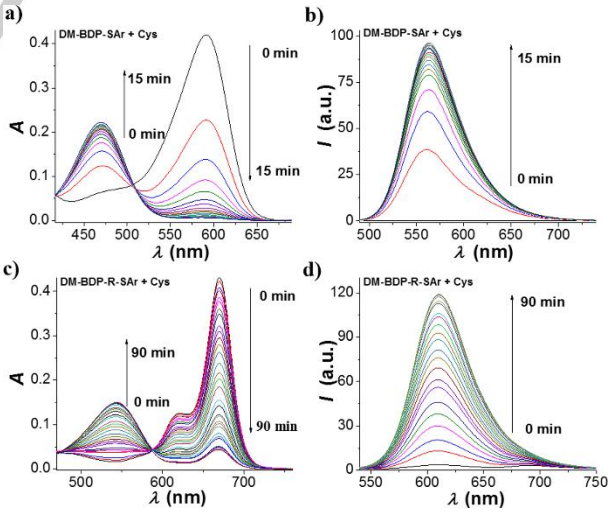

Figure 1. Time-dependent absorption and fluorescence spectra of probes (10 μM) in the presence of 10 equiv. of Cys in acetonitrile/PBS buffer (1 : 1, v/v, 10 mM, pH 7.4) at 37 °C. (a) Absorption spectra and (b) fluorescence spectra (λ_{ex} = 465 nm) of **DM-BDP-SAr** treated with Cys; (c) Absorption spectra and (d) fluorescence spectra (λ_{ex} = 525 nm) of **DM-BDP-R-SAr** after addition of Cys. The excitation and emission slit widths are set at 1 nm.

reached, which was very unusual for BODIPY dyes wherein small Stokes' shift was characteristic.[14,50,51] These unexpected and unusual properties were obviously induced by the aryl moieties which may squeeze the 1,7-dimethyl positions to block the attack of the *meso* position by Hcy/GSH. As a reasonable assumption, conformationally restricted **DM-BDP-R-SAr** should be more difficult to the attack of thiol. Therefore, when **DM-BDP-R-SAr** was used for the detection of Cys, surprisingly over 90 min was required to reach complete response (Figure 1c and 1d). **DM-BDP-R-SAr** was also reluctant to react with Hcy or GSH (Figure S2). Much diminished reacting rate of **DM-BDP-R-SAr** compared to **DM-BDP-SAr** supported our assumption that the more steric repulsion of the fused ring enhanced the steric congestion of the 1,7-dimethyl moieties, which can also be confirmed by the reduced reaction rate of conformationally restricted probe to Cys and Hcy in our group's previous studies (**Scheme 1c)**.[48]

Mechanistic Investigations

Based on the spectroscopic changes in comparison with general rational observed,[43-48] the Cys selective responses of both probes were attributed to the Cys-induced S_NAr substitution-rearrangement reaction to generate *meso*-amino-BODIPYs. The low fluorescence of **DM-BDP-SAr** or **DM-BDP-R-SAr** was initially thought to be induced by photoinduced electron transfer (PET) as demonstrated in previous publications (Scheme 4a).[52-54] However, when density functional theory (DFT) calculation were performed on **DM-BDP-SAr** and **DM-BDP-N-Cys** (Figure S3), it was astonishingly found that electron densities of both HOMO and LUMO orbitals mostly localized on the acceptor (BODIPY moiety) and the spin-orbit coupling (SOC) values are 1.28 cm^{-1} the $S_1 \rightarrow T_1$ and 6.37 cm^{-1} for $S_2 \rightarrow T_1$ of **DM-BDP-SAr**, 18.3 and 12.5 times larger than those data of **DM-BDP-N-Cys** (the SOC value of $S_1 \rightarrow T_1$ and $S_2 \rightarrow T_1$ for **DM-BDP-N-Cys** are 0.07 cm^{-1} and 0.51 cm^{-1} respectively). Therefore, it was possible that intersystem crossing (leading to the high population of T_1) dominated the decay which led to the low fluorescence of the probe.[55] The modified mechanism based on DFT calculation was shown in Scheme 4b.

To find evidences for the mechanism of Scheme 4b, HRMS studies were performed to monitor the reaction of **DM-BDP-SAr**/**DM-BDP-R-SAr** with Cys. In the presence of Cys, **DM-BDP-SAr** generated a species with characteristic peak at m/z = 552.1943 corresponding to the **DM-BDP-N-Cys** $[M+H]^+$ (Figure S4), while **DM-BDP-R-SAr** produced a characteristic peak at m/z = 604.2247 corresponding to the **DM-BDP-R-N-Cys** $[M+H]^+$ (Figure S5). An evidence for the intersystem crossing is the increased rate of generation of $^1O_2$. Enhancement of spin-orbit interaction is a popular way to convert BODIPY fluorophore into photosensitizer.[56] When 1,3-diphenylisobenzofuran (DPBF, a known efficient quencher of singlet oxygen) was used to trap singlet oxygen produced of **DM-BDP-SAr** under illumination of light >500 nm using ZnPc as standard (Φ_Δ of 0.56 in DMF) (Figure S6), the singlet oxygen quantum yield (Φ_Δ) was calculated to be 0.31. In comparison, a BODIPY dye with *meso* chloro substitutent (**BDP-Cl**) only provided Φ_Δ of 0.06. Therefore, the high population of T_1 in **DM-BDP-R-SAr** could be reasonably attributed to cause the fluorescence quenching.

So far, we have established supporting evidences for the plausible mechanism of both **DM-BDP-SAr** and **DM-BDP-R-SAr** for the selective response to Cys with **DM-BDP-SAr** to be a preferred one. We therefore further pursued to apply the current system into a lysosome-targeted version. Such efforts were accessed through the attachment of morpholinoethoxy group(s) onto the *para*-position of one or two phenyl moieties (Scheme 2b). The designed lysosome targeting probes were prepared similarly as **DM-BDP-SAr** as indicated in Scheme 3. The responsive behaviors and targeting abilities of **Lyso-S** and **Lyso-D** were investigated afterwards.

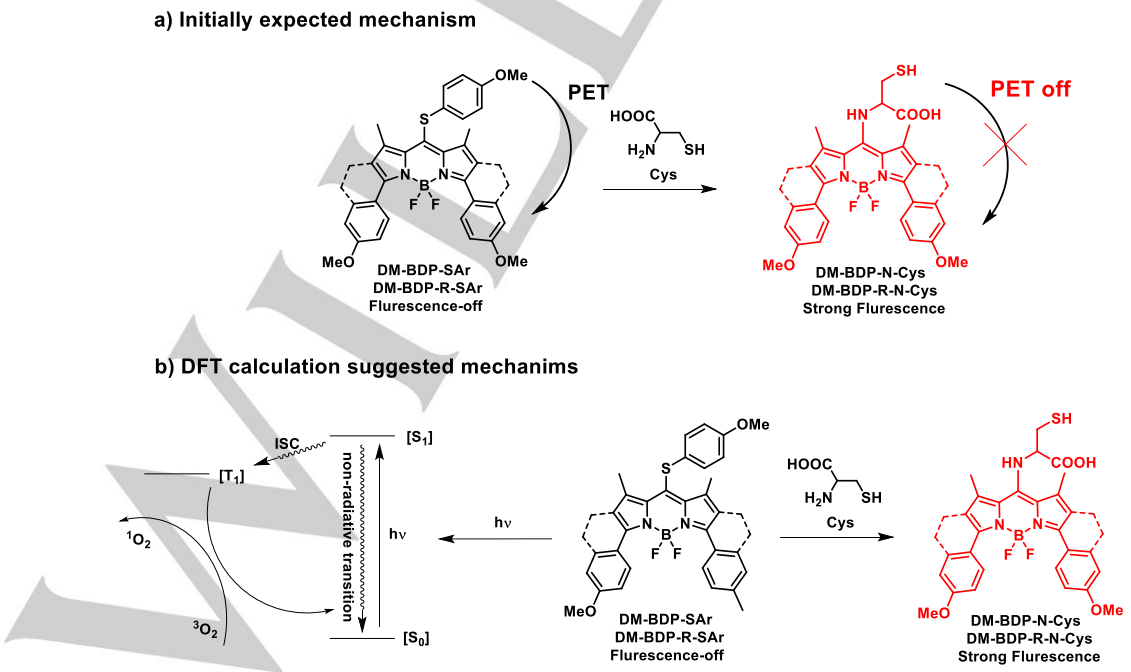

Scheme 4 Proposed sensing mechanism of **DM-BDP-R-SAr** and **DM-BDP-SAr** for Cys.

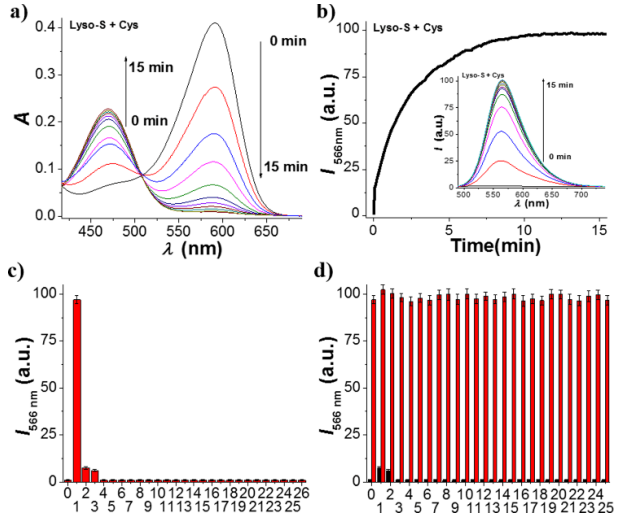

Figure 2. Spectroscopic data measured for **Lyso-S** (10 μM) in acetonitrile/PBS buffer (1 : 1, v/v, 10 mM, pH 7.4, λ_{ex} = 465 nm) at 37 °C. (a) Time-dependent absorption spectra changes upon treatment with 10 equiv. of Cys; (b) Time-dependent fluorescence intensity changes and spectra changes (inset) upon treatment with 10 equiv. of Cys (λ_{ex} = 465 nm); (c) Fluorescence intensities monitored at 566 nm upon treatment with 100 μM of individual analyte for 15 min. (0) Blank, (1) Cys, (2) Hcy, (3) GSH, (4) Ala, (5) Arg, (6) Asp, (7) Gla, (8) Gln, (9) Glu, (10) Gly, (11) His, (12) Ile, (13) Leu, (14) Lys, (15) Met, (16) Phe, (17) Pro, (18) Ser, (19) Thr, (20) Try, (21) NaSH, (22) HSO_3^-, (23) SO_3^{2-}, (24) $S_2O_3^{2-}$, (25) $S_2O_4^{2-}$, (26) $S_2O_5^{2-}$; (d) Fluorescence intensities (black bars) upon treatment with individual analyte (100 μM) for 15 min in comparison with those (red bars) after addition of Cys (100 μM). (0) Blank, (1) Hcy, (2) GSH, (3) Ala, (4) Arg, (5) Asp, (6) Gla, (7) Gln, (8) Glu, (9) Gly, (10) His, (11) Ile, (12) Leu, (13) Lys, (14) Met, (15) Phe, (16) Pro, (17) Ser, (18) Thr, (19) Try, (20) NaSH, (21) HSO_3^-, (22) SO_3^{2-}, (23) $S_2O_3^{2-}$, (24) $S_2O_4^{2-}$, (25) $S_2O_5^{2-}$. The excitation and emission slit widths are set at 1 nm and Error bars are relative standard deviations (RSD), n=3.

Time-dependent spectral changes of Lyso-S and Lyso-D with Cys

We first examined the time-dependent responses on absorption and emission behaviours of **Lyso-S** and **Lyso-D** to Cys, respectively. The absorption maximum of **Lyso-S** was 592 nm and **Lyso-S** exhibited fairly low fluorescence at 624 nm under excitation with light of 465 nm. Upon addition of Cys in acetonitrile/PBS buffer (1 : 1, v/v, 10 mM, pH 7.4) at 37 °C, the absorption at 592 nm decreased abruptly, accompanied by an increase in the absorption at 469 nm displaying significant hypsochromic shift (123 nm, Figure 2a). Meanwhile, a new fluorescence band centered at 566 nm illustrated dramatic increment of fluorescence up to 113-fold over the intrinsic fluorescence of **Lyso-S** in 15 min (Figure 2b). For **Lyso-D**, similar trend was also observed as shown in Figure S7a and S7b. These results indicated that both **Lyso-S** and **Lyso-D** exhibit fast responses to Cys, which would be favorable for the detection of Cys in the living systems.

Selective responses of Lyso-S and Lyso-D to Cys

To evaluate the selectivity of **Lyso-S**/**Lyso-D**, Hcy and GSH were measured for the fluorescence changes upon reacting with the probes (Figure 2c, Figure S8 and Figure S9). It was found that neither **Lyso-S**, nor **Lyso-D** showed significant spectroscopic changes with Hcy/GSH. The selectivity patterns for **Lyso-S** and **Lyso-D** were further examined with various amino acids as well as various sulfur-containing inorganic anion species.

With the excitation of 465 nm, the fluorescence monitored at 566 nm indicated that no obvious fluorescence enhancement for **Lyso-S** could be triggered by the treatment of various amino acids, as well as various sulfur-containing inorganic anion species (Figure 2c). To further demonstrate the selective recognition of **Lyso-S** to Cys, the competition experiments were also carried out by addition of Cys to the solution of **Lyso-S** in the presence of other analytes. As shown in Figure 2d, the co-existence of other analytes did not have obvious impact on **Lyso-S** to detection of Cys. Interfering investigation and competition experiments on **Lyso-D** also demonstrated selective responses to Cys (Figure S10).

Considering that ROS/RNS species may potentially oxidize thioethers,[57-62] the interference of ROS/RNS to the detection of Cys was also evaluated and the results were collected in Figure S11. It can be clearly seen that the detection of Cys with our probes (**Lyso-S** and **Lyso-D**) was not affected by ROS/RNS species.

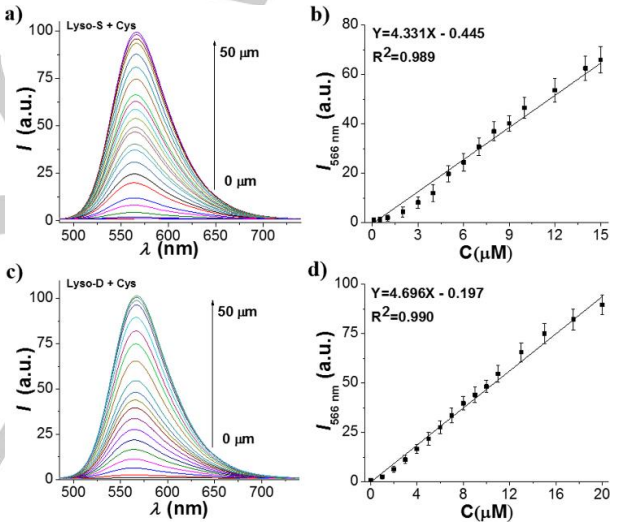

Figure 3. Fluorescence spectral changes of (a) **Lyso-S** and (c) **Lyso-D** upon addition of increased concentrations of Cys (10 μM, λ_{ex} = 465 nm). Each spectrum was recorded 15 min after Cys addition in acetonitrile/PBS buffer (1 : 1, v/v, 10 mM, pH 7.4) at 37 °C; A linear relationship of fluorescence intensity changes at 566 nm of (b) **Lyso-S** and (d) **Lyso-D** against Cys concentration, which can be linearly fitted by the equation Y = 4.331 X – 0.445, with R^2 = 0.990 and Y = 4.696 X – 0.197, with R^2 = 0.989 respectively. The excitation and emission slit widths are set at 1 nm and Error bars are relative standard deviations (RSD), n=3.

The sensitivities of probes toward various concentrations of Cys

To check whether **Lyso-S** and **Lyso-D** fluorescence response changes over Cys concentration, the Cys titration experiments of these two probes were measured (Figure 3). Figures 3a and 3c shows the changes in the emission of **Lyso-S** and **Lyso-D** in the presence of increasing concentration of Cys. Further studies suggested a concentration-dependent response manner with the linear response of **Lyso-S** toward Cys ranging from 0 μM to 15

μM and the detection limit was estimated as 46 nM (Figure 3b), while **Lyso-D** showed a linear response toward Cys ranging from 0 μM to 20 μM and the detection limit was estimated as 76 nM (Figure 3d).

The effect of pH

The effect of the pH value on the fluorescence behaviors of **Lyso-S** and **Lyso-D** toward Cys were carried out as well and the data were collected in Figure S12. Both the probes of **Lyso-S** and **Lyso-D** were fairly stable in pH range of 4.0–8.0 with very low fluorescence emission. In the presence of Cys, noticeable fluorescence enhancement at pH range from 4.8 to 8.0 was observed. The increased reactivity towards Cys was observed along with increased pH value for both probes. These observations correlated well with the previous reports ascribed to the larger concentration of thiolate species in higher pH environment.[12-31] Lysosomes are spherical-shaped, catabolic organelles with an acidic interior (pH 4.0–6.0).[63] Though diminished reactivity towards Cys was found, both **Lyso-S** and **Lyso-D** could function properly under lysosomal pH environment.

Bioimaging applications of Lyso-S and Lyso-D

To further assess the biological application with our probes, toxicity studies performed on HeLa cells via MTT for both **Lyso-S** and **Lyso-D** (Figure S13). The results suggested that both probes lack of toxicity up to 20 μM. Then, confocal laser scanning microscopic fluorescence imaging was used to examine the capability of **Lyso-S** and **Lyso-D** to detect Cys in living cells (Figures 4 and S14). Bright red fluorescence could be visualized in HeLa cells upon addition of **Lyso-S** and **Lyso-D** respectively after incubated for 30 min. By contrast, when HeLa cells were pre-treated with 5 mM of NEM, a well-known scavenger of biothiols,[64] for 30 min and subsequently incubated with **Lyso-S** and **Lyso-D**, only weak red fluorescence was noticed. The result exhibits that **Lyso-S** and **Lyso-D** could sense intracellular Cys from red emission channels, which are favourable to bioimaging applications due to the reduced background of absorption, fluorescence, and light scattering in long wavelength region.[65-67]

Next, the colocalization experiments were performed by co-staining **Lyso-S** with various commercially available organelle-tracing probes such as Lyso-Tracker Green DND-26, Mito-Tracker Green, as well as Hoechst (a nucleus-specific dye) in HeLa cells to figure out the location of the probe. As shown in Figure 5, good overlap of the red emission from **Lyso-S** with the green emission from Lyso-Tracker Green DND-26 was observed from the merged image shown in the yellow color, the Pearson's colocalization coefficient calculated from the intensity correlation plots was 0.79. The intensity profiles of the linear regions of

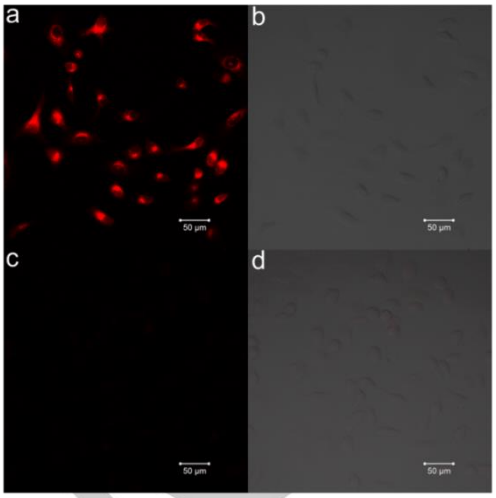

Figure 4. Confocal fluorescence and bright-field images of living HeLa cells. (a) fluorescence and (b) bright field images of HeLa cells after incubated with **Lyso-S** (10 μM) for 30 min; (c) fluorescence and (d) bright field images of HeLa cells pretreated with 5 mM of NEM for 30 min and then incubated with **Lyso-S** (10 μM) for 30 min. All fluorescence was taken in red channel at 580−620 nm in identical conditions.

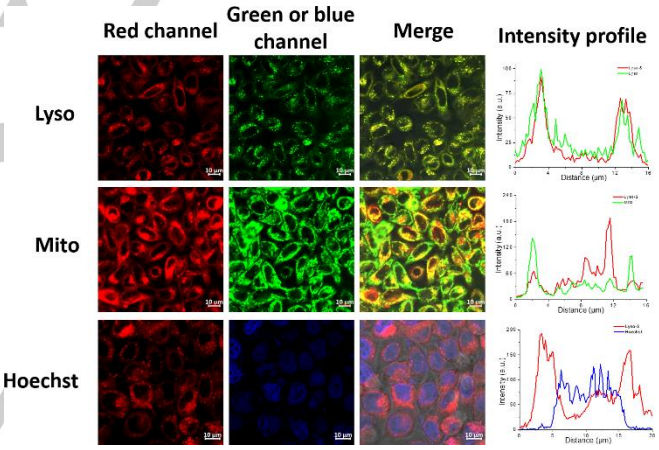

Figure 5. Confocal laser scanning microscopic images for intracellular localization of **Lyso-S** in HeLa cells. Cells were treated with 10 μM **Lyso-S** for 30 min and co-stained with 100 nM Lyso-Tracker DND-26, 200 nM Mito-Tracker Green, or 5 μg/mL Hoechst respectively. Red channel at 580−620 nm. Green channel at 490−520 nm for Lyso-Tracker Green DND-26 and Mito-Tracker Green, 440−480 nm for Hoechst.

interest (ROI) across HeLa cells stained with **Lyso-S** and Lyso-Tracker Green DND-26 vary in close synchrony. Comparatively, no good overlap was observed between **Lyso-S** and Mito-Tracker Green or Hoechst. These results confirmed the majority of **Lyso-S** localized within lysosomes of the cells and suggested the potential of **Lyso-S** as a probe for the detection of Cys in lysosome of living HeLa cells. Similarly, the colocalization experiments of **Lyso-D** co-stained with Lyso-Tracker Green DND-26, Mito-Tracker Green, and Hoechst demonstrated that **Lyso-D** could also efficiently localized in the lysosomes (Pearson's colocalization coefficient was 0.78) to selective detection Cys in living HeLa cells (Figure S15). Therefore, both **Lyso-S** and **Lyso-D** in the lysosomes to selective detect Cys in living HeLa cells could be achieved. It is also revealed that one morpholino group is sufficient to provide the lysosome targeting.

Additional morpholine moiety did not further enhance the targeting capability.

Conclusions

In an attempt to design new long wavelength fluorescent probes to detect biothiol species in dual emission mode through *meso* replacement, we attached aromatic moiety at 3 and 5 positions of BODIPY dye with 1,7-dimethyl to control the replacement and obtained **DM-BDP-SAr** and **DM-BDP-R-SAr**. The expected dual emission detection was not reached and unexpected selective detection to Cys over Hcy/GSH was found with enormous 100 nm Stokes' shift. **DM-BDP-SAr** turned out to be a preferred probe for Cys with faster reaction rate. We further modified the probe with lysosomal targeting morpholine moiety and developed **Lyso-S** and **Lyso-D** as selective probes for Cys detection in lysosome. Good linear responses ranged from 0 μM to 15 μM with the detection limit of 46 nM for **Lyso-S**, and 0—20 μM (with a detection limit of 76 nM) for **Lyso-D** were reached. As desired, both **Lyso-S** and **Lyso-D** could localize in lysosomes nicely. Moreover, a novel fluorescence quenching mechanism was proposed based on density functional theory (DFT) calculation. The probes showed significant intersystem crossing in the excited state (from singlet to triplet excited states) which induced fluorescence quenching.

Experimental Section

Ethyl 2-(hydroxyimino)-3-oxobutanoate, **1a–1c, 2a–2c, 3a–3c** and **4c** were prepared according the reported methods.[68-72]

Ethyl 7-methoxy-3-methyl-4,5-dihydro-1H-benzo[g]indole-2-carboxylate (1a). In a 1000 mL flask, 6-methoxytetralone (19.4 g, 110 mmol) and sodium acetate (54.0 g, 660 mmol) were dissolved in propionic acid (300 mL). When the mixture was heated to 150 °C, a solution of compound 1a (17.5 g, 110 mmol) in 200 mL propionic acid and zinc dust (71.0 g, 1.10mol) were slowly added to the stirred mixture at 150 °C. After the addition, the mixture was stirred at 150 °C for 2 h and cooled to about 70 °C. It was then poured into ice/water mixture and was allowed to stand overnight. The precipitate was filtered and washed with water until the pH value of filtrate was 7.0. The residue was then recrystallized from ethanol several times to give compound **1a** (4.6 g, 15%) as a white solid. ^{1}H-NMR (400 MHz, $CDCl_3$): δ 9.20 (s, 1H), 7.32 (d, J = 8.3 Hz, 1H), 6.87–6.71 (m, 2 H), 4.35 (q, J = 7.1 Hz, 2H), 3.82 (s, 3H), 2.92 (t, J = 7.5 Hz, 2H), 2.64 (t, J = 7.5 Hz, 2H), 2.30 (s, 3H), 1.38 (t, J = 7.1 Hz, 3H).

7-Methoxy-3-methyl-4,5-dihydro-1H-benzo[g]indole (1b). NaOH (0.40 g, 10 mmol) and compound **1a** (0.70 g, 2.5 mmol) were added to ethylene glycol (40 mL) and heated to 160 °C under nitrogen. After stirring at 160 °C for 2 h, the reaction mixture was treated with saturated NaCl solution and the resulting solution was extracted with CH_2Cl_2. The extract was washed with H_2O and brine, dried with anhydrous Na_2SO_4, filtered and evaporated. The purification of the crude product was carried out by silica gel column chromatography (CH_2Cl_2/petroleum ether, 1 : 1, v/v) to yield white powder (0.27 g, 50%). ^{1}H-NMR (400 MHz, $CDCl_3$): δ 8.00 (s, 1H), 7.05 (d, J = 8.3 Hz, 1H), 6.81 (d, J = 2.3 Hz 1 H), 6.72 (dd, J = 8.3 ,2.5 Hz, 1H), 6.51 (s, 1H), 3.81 (s, 3H), 2.93 (t, J = 7.6 Hz, 2H), 2.66 (t, J = 7.6 Hz, 2H), 2.08 (s, 3H).

Bis(7-methoxy-3-methyl-4,5-dihydro-1H-benzo[g]indol-2-yl)methanone (1c). A solution of triphosgene (0.90 g, 3.1 mmol) in THF (30 mL) was added to a stirred solution of compound **1b** (1.0 g, 4.7 mmol) and ethyldiisopropylamine (0.70 mL, 4.7 mmol) in THF (10 mL) over 20 min at 0 °C under nitrogen. After stirred for 2 h at 0 °C, the reaction mixture was treated with saturated NaCl solution and the resulting solution was extracted with CH_2Cl_2. The extract was washed with H_2O and brine, dried with anhydrous Na_2SO_4, filtered and evaporated. The purification of the crude product was carried out by silica gel column chromatography (CH_2Cl_2/ethyl acetate, 6 : 1, v/v) to yield yellow solid (0.42 g, 40%). ^{1}H-NMR (400 MHz, d_6-DMSO): δ 11.46 (s, 2H), 7.78 (d, J = 8.5 Hz, 2H), 6.84 (d, J = 2.3 Hz 2 H), 6.78 (dd, J = 8.5 ,2.5 Hz, 2H), 3.75 (s, 6H), 2.86 (t, J = 7.5 Hz, 4H), 2.58 (t, J = 7.4 Hz, 4H), 2.04 (s, 6H).

Compound 1d. Compound **1c** (0.30 g, 0.66 mmol) was dissolved in 1,2-dichloroethane (10 mL). Phosphorus oxychloride (0.30 mL, 2.6 mmol) was added at 0 °C under nitrogen, and the reaction mixture was allowed to come to room temperature and stirred for 12 h, then cooled in an ice bath. Triethylamine (0.60 mL, 4.0 mmol) was added, and the reaction was stirred at 0 °C for 5 min. Boron trifluoride etherate (0.70 mL, 5.3 mmol) was added dropwise while maintaining the temperature at 0 °C. The reaction mixture was allowed to come to room temperature and stirred for an additional 30 min. The resulting solution was poured out in diethyl ether (300 mL) and extracted with water. After drying over Na_2SO_4, filtration, and evaporation, the crude product was purified by silica gel column chromatography (CH_2Cl_2/petroleum ether, 1 : 1, v/v) to yield mazarine solid (0.12 g, 35%). ^{1}H-NMR (400 MHz, $CDCl_3$): δ 8.69 (d, J = 8.9 Hz, 2H, 3,5-ArH), 6.95 (dd, J = 8.9, 2.5 Hz, 2H, 3,5-ArH), 6.80 (s, 2 H, 3,5-ArH), 3.87 (s, 6H, 3,5-Ar-OCH_3), 2.88 (t, J = 6.2 Hz, 4H, -CH_2CH_2-), 2.64 (t, J = 6.1 Hz, 4H, -CH_2CH_2-), 2.47 (s, 6H, 1,7-CH_3); ^{13}C-NMR (100 MHz, $CDCl_3$): δ 160.57; 149.83; 143.09; 135.10; 132.28; 131.69; 131.21; 130.30; 121.21; 114.16; 112.27.

DM-BDP-R-SAr. Compound **1d** (52 mg, 0.10 mmol) was dissolved in CH_2Cl_2 (50 mL), p-methoxythiophenol (70 mg, 0.50 mmol) and NEt_3 (51 mg, 0.50 mmol) were added. The reaction mixture was purged with nitrogen and stirred at room temperature for 2 h. The crude mixture was poured out in diethyl ether, washed with aqueous Na_2CO_3, and the organic layer was evaporated to dryness. **DM-BDP-R-SAr** was obtained as a brown solid (55 mg, 88%) after filtration over a silica gel column chromatography (CH_2Cl_2/petroleum ether, 2 : 1, v/v). M. P. > 300 °C; ^{1}H-NMR (400 MHz, $CDCl_3$): δ 8.71 (d, J = 9.0 Hz 2H, 3,5-ArH), 7.19 (d, J = 8.8 Hz, 2H, 8-ArH), 6.94 (dd, J = 8.9, 2.6 Hz, 2H, 3,5-ArH), 6.83 (d, J = 8.9 Hz, 2H, 8-ArH), 6.79 (d, J = 2.5 Hz, 2H, 3,5-ArH), 3.87 (s, 6H, 3,5-Ar-OCH_3), 3.76 (s, 3H, 8-Ar-OCH_3), 2.86 (t, J = 6.9 Hz, 4H, -CH_2CH_2-), 2.58 (t, J = 6.5 Hz, 4H, -CH_2CH_2-), 2.43 (s, 6H, 1,7-CH_3); ^{13}C-NMR (100 MHz, $CDCl_3$): δ 160.61; 158.01; 150.51; 143.33; 137.13; 136.28; 131.75; 130.57; 129.85; 128.43; 127.66; 121.38; 115.20; 114.12; 112.28; 55.32; 30.84; 29.73; 20.57; 14.62. HRMS-MALDI: Calculated for $[C_{36}H_{33}BF_2N_2O_3S]^+$: 621.2278; found 621.2303.

Bis(5-(4-methoxyphenyl)-3-methyl-1H-pyrrol-2-yl)methanone (2c). The synthesis of compound **2c** was analogous to the synthesis of compound **1c** starting from 2-(4'methoxyphenyl)-4-methyl pyrrole **(2b)**. ^{1}H-NMR (400 MHz, $CDCl_3$): δ 9.05 (s, 2H), 7.58–7.43 (m, 4H), 6.94 (d, J = 8.8 Hz, 4H), 6.37 (s, 2H), 3.84 (s, 6H), 2.31 (s, 6H).

8-Chloro-1,7-dimethyl-3,5-di(p-methoxyphenyl)-4,4-difluoro-4-bora-3a,4a-diaza-s-indacene (2d). The synthesis of compound **2d** was analogous to the synthesis of compound **1d**. ^{1}H-NMR (400 MHz, $CDCl_3$): δ 7.78 (d, J = 8.8 Hz, 4H, 3,5-ArH), 6.92 (d, J = 8.9 Hz, 4H, 3,5-ArH), 6.41 (s, 2H, Pyrrole-H), 3.83 (s, 6H, 3,5-Ar-OCH_3), 2.56 (s, 6H, 1,7-CH_3); ^{13}C-NMR (100 MHz, $CDCl_3$): δ 160.63, 155.81, 142.51, 136.58, 131.27, 131.04, 124.80, 122.83, 113.68, 55.31, 17.26.

DM-BDP-SAr. The synthesis of **DM-BDP-SAr** was analogous to the synthesis of **DM-BDP-R-SAr**. M. P. 186–188 °C; ^{1}H-NMR (400 MHz, $CDCl_3$): δ 7.79 (d, J = 8.8 Hz, 4H, 3,5-ArH), 7.21 (d, J = 8.8 Hz, 2H, 8-ArH), 6.92 (d, J = 8.8 Hz, 4H, 3,5-ArH), 6.86 (d, J = 8.8 Hz, 2H, 8-ArH), 6.36 (s, 2H, Pyrrole-H), 3.83 (s, 6H, 3,5-Ar-OCH_3), 3.77 (s, 3H, 8-Ar-OCH_3), 2.51 (s, 6H, 1,7-CH_3); ^{13}C-NMR (100 MHz, $CDCl_3$): δ 160.63; 158.31; 156.36; 143.64; 136.32; 135.57; 131.10; 128.11; 127.45; 125.09; 123.36; 115.32; 113.66; 55.29; 29.73; 17.62. HRMS-MALDI: Calculated for $[C_{32}H_{29}BF_2N_2O_3S]^+$: 569.2005; found 569.1991.

2-(4'-Morpholineethoxyphenyl)-4-methyl pyrrole (3b). The synthesis of compound **3b** was analogous to the synthesis of compound **1b**. ^{1}H-NMR (400 MHz, $CDCl_3$): δ 8.31 (s, 1H), 7.35 (d, J = 8.7 Hz, 2H), 6.88 (d, J = 8.7 Hz, 2H), 6.56 (s, 1H), 6.26 (s, 1H), 4.11 (t, J = 5.7 Hz, 2H), 3.78–3.72 (m, 4H), 2.81 (t, J = 5.7 Hz, 2H), 2.64–2.56 (m, 4H), 2.16 (s, 3H).

(5-(4-Methoxyphenyl)-3-methyl-1H-pyrrol-2-yl)(3-methyl-5-(4-(2-morpholinoethoxy)phenyl)-1H-pyrrol-2-yl)methanone (3c). A solution of triphosgene (0.30 g, 1.0 mmol) in 1,2-dichloroethane (10 mL) was added to a stirred solution of compound **2b** (561 mg, 3 mmol) and ethyldiisopropylamine (0.50 mL, 3.0 mmol) in 1,2-dichloroethane (10 mL) over 10 min at 0 °C under nitrogen. After stirred for 1 h at 0 °C, the compound **3b** (0.86 g, 3.0 mmol) was added. The reaction mixture was stirred at 35 °C for 4 h. Then, the reaction mixture was treated with saturated NaCl solution and the resulting solution was extracted with CH_2Cl_2. The extract was washed with H_2O and brine, dried with anhydrous Na_2SO_4, filtered and evaporated. The purification of the crude product was carried out by silica gel column chromatography (CH_2Cl_2/ethyl acetate, 3 : 1, v/v) to yield yellow solid (0.53 g, 35%). ^{1}H-NMR (400 MHz, $CDCl_3$): δ 7.84–7.70 (m, 4H), 6.91 (d, J = 8.5 Hz, 4H), 6.41 (d, J = 10.4 Hz, 2H), 4.39 (s, 2H), 3.95 (s, 4H), 3.83 (s, 3H), 3.16 (s, 2H), 2.99 (s, 4H), 2.57 (s, 6H).

8-Chloro-1,7-dimethyl-3-(p-methoxyphenyl)-5-(p-morpholinoethoxyphenyl)-4,4-difluoro-4-bora-3a,4a-diaza-s-indacene (3d). The synthesis of compound **3d** was analogous to the synthesis of compound **1d**. ^{1}H-NMR (400 MHz, $CDCl_3$): δ 7.77 (dd, J = 8.8, 3.7 Hz, 4H, 3,5-ArH), 6.91 (d, J = 8.8 Hz, 4H, 3,5-ArH), 6.40 (s, 2H, Pyrrole-H), 4.12 (t, J = 5.6 Hz, 2H, -ArOCH_2-), 3.81 (s, 3H, 3-Ar-OCH_3), 3.77–3.71 (m, 4H, -$O(CH_2)_2$), 2.80 (t, J = 5.6 Hz, 2H, -CH_2N-), 2.61–2.51 (m, 10H, -$N(CH_2)_2$ and 1,7-CH_3); ^{13}C-NMR (100 MHz, $CDCl_3$): δ 160.70; 159.78; 155.92; 155.71; 142.56; 142.45; 136.59; 131.32; 131.05; 125.02; 124.80; 122.83; 114.25; 113.69; 66.89; 65.71; 57.54; 55.27; 54.05; 17.17.

Lyso-S. The synthesis of **Lyso-S** was analogous to the synthesis of **DM-BDP-R-SAr**. M. P. 110–-113 °C; ^{1}H-NMR (400 MHz, $CDCl_3$): δ 7.79 (dd, J = 8.6, 4.1 Hz, 4H, 3,5-ArH), 7.21 (d, J = 8.7 Hz, 2H, 8-ArH), 6.91 (d, J = 8.7 Hz, 4H, 3,5-ArH), 6.86 (d, J = 8.7 Hz, 2H, 8-ArH), 6.36 (d, J = 2.7 Hz, 2H, Pyrrole-H), 4.15 (t, J = 5.5 Hz, 2H, -ArOCH_2-), 3.82 (s, 3H, 3-Ar-OCH_3), 3.80–3.73 (m, 7H, 8-Ar-OCH_3 and -$O(CH_2)_2$), 2.82 (t, J = 5.5 Hz, 2H, -CH_2N-), 2.60 (s, 4H, -$N(CH_2)_2$), 2.51 (s, 6H, 1,7-CH_3); ^{13}C-NMR (100 MHz, $CDCl_3$): δ 160.71; 159.73; 158.36; 156.45; 156.20; 143.72; 143.59; 136.40; 136.31; 135.69; 131.10; 128.12; 127.48; 125.35; 125.09; 123.41; 123.34; 115.35; 114.21; 113.66; 66.83; 65.65; 57.54; 55.38; 55.27; 54.02; 17.60; HRMS-MALDI: Calculated for $[C_{37}H_{38}BF_2N_3O_4SNa]^+$: 691.2596; found 691.2573.

Bis(3-methyl-5-(4-(2-morpholinoethoxy)phenyl)-1H-pyrrol-2-yl)methanone (4c). The synthesis of compound **4c** was analogous to the synthesis of compound **1c**. Only the characterization data was given here. ^{1}H-NMR (400 MHz, $CDCl_3$): δ 9.96 (s, 2H), 7.45 (d, J = 8.5 Hz, 4H), 6.82 (d, J = 8.6 Hz, 4H), 6.30 (s, 2H), 4.02 (t, J = 5.5 Hz, 4H), 3.72–3.67 (m, 8H), 2.73 (t, J = 5.5 Hz, 4H), 2.53 (d, J = 3.9 Hz, 8H), 2.22 (s, 6H).

8-Chloro-1,7-dimethyl-3,5-di(p-morpholinoethoxypheny)l-4,4-difluoro-4-bora-3a,4a-diaza-s-indacene (4d). The synthesis of compound **4d** was analogous to the synthesis of compound **1d**. Only the characterization data were given here. ^{1}H-NMR (400 MHz, $CDCl_3$): δ 7.75 (d, J = 8.7 Hz, 4H, 3,5-ArH), 6.90 (d, J = 8.7 Hz, 4H, 3,5-ArH), 6.40 (s, 2H, Pyrrole-H), 4.14 (t, J = 5.5 Hz, 4H, -ArOCH_2-), 3.77–3.71 (m, 8H, -$O(CH_2)_2$), 2.83 (t, J = 5.5 Hz, 4H, -CH_2N-), 2.62 (d, J = 3.9 Hz, 8H, -$N(CH_2)_2$), 2.56 (s, 6H, 1,7-CH_3); ^{13}C-NMR (100 MHz, $CDCl_3$): δ 159.69; 155.76; 142.56; 136.70; 131.30; 131.04; 125.06; 122.81; 114.23; 66.73; 65.56; 57.49; 53.97; 17.17.

Lyso-D. The synthesis of **Lyso-D** was analogous to the synthesis of **DM-BDP-R-SAr**. Only the characterization data were given here. M. P. 92–95 °C; ^{1}H-NMR (400 MHz, $CDCl_3$): δ 7.77 (d, J = 8.8 Hz, 4H, 3,5-ArH), 7.20 (d, J = 8.8 Hz, 2H, 8-ArH), 6.90 (d, J = 8.8 Hz, 4H, 3,5-ArH), 6.86 (d, J = 8.9 Hz, 2H, 8-ArH), 6.35 (s, 2H, Pyrrole-H), 4.14 (t, J = 5.6 Hz, 4H, -ArOCH_2-), 3.77 (s, 3H, 8-Ar-OCH_3), 3.76–3.71 (m, 8H, -$O(CH_2)_2$), 2.81 (t, J = 5.6 Hz, 4H, -CH_2N-), 2.63–2.55 (m, 8H, -$N(CH_2)_2$), 2.51 (s, 6H, 1,7-CH_3); ^{13}C-NMR (100 MHz, $CDCl_3$): δ 159.78; 158.36; 156.28; 143.67; 136.35; 135.75; 131.10; 128.12; 127.46; 125.29; 123.37; 115.35; 114.20; 66.90; 65.73; 57.57; 55.38; 54.06; 17.58; HRMS-MALDI: Calculated for $[C_{42}H_{47}BF_2N_4O_5SNa]^+$: 791.3232; found 791.3220.

Acknowledgements

This research was supported by the National Natural Science Foundation of China (No. 21372063, No. 21702046, No. 21703077) and Project Funded by China Postdoctoral Science Foundation (2018M632757). The authors thank Dr. Weiwei

Zhang for his helpful disscussions in the density functional theory (DFT) calculation.

Keywords: BODIPY • fluorescent probe • cysteine • lysosome-targeted

[1] Z. A. Wood, E. Schröder, J. R. Harris, L. B. Poole, *Trends Biochem. Sci.* **2003**, *28*, 32-40.
[2] H. Refsum, A. D. Smith, P. M. Ueland, E. Nexo, R. Clarke, J. McPartlin, C. Johnston, F. Engbaek, J. Schneede, C. McPartlin, J. M. Scott, *Clin. Chem.* **2004**, *50*, 3-32.
[3] J. Keelan, N. J. Allen, D. Antcliffe, S. Pal, M. R. Duchen, *J. Neurosci. Res.* **2001**, *66*, 873-884.
[4] D. M. Townsend, K. D. Tew, H. Tapiero, *Biomed. Pharmacother.* 2003, **57**, 145-155.
[5] J. S. Armstrong, K. K. Steinauer, B. Hornung, J. M. Irish, P. Lecane, G. W. Birrell, D. M. Peehl, S. J. Knox, *Cell Death Differ.* **2002**, *9*, 252-263.
[6] T. P. Dalton, H. G. Shertzer, A. Puga, *Annu. Rev. Pharmacol. Toxicol.* **1999**, *39*, 67-101.
[7] B. Arunachalam, U. T. Phan, H. J. Geuze, P. Cresswell, *Proc. Nat. Acad. Sci. U. S. A.* **2000**, *97*, 745-750.
[8] D. R. Balce, E. R. Allan, N. McKenna, R. M. Yates, *J. Biol. Chem.* **2014**, *289*, 31891-31904.
[9] D. Kand, T. Saha, M. Lahiri, P. Talukdar, *Org. Biomol. Chem.* **2015**, *13*, 8163-8168.
[10] J. Fan, Z. Han, Y. Kang, X. Peng, *Sci. Rep.* **2016**, *6*, 19562-19569.
[11] Q. Gao, W. Zhang, B. Song, R. Zhang, W. Guo, J. Yuan, *Anal. Chem.* **2017**, *89*, 4517-4524.
[12] C. Yin, F. Huo, J. Zhang, R. Martinez-Manez, Y. Yang, H. Lv, S. Li, *Chem. Soc. Rev.* **2013**, *42*, 6032-6059.
[13] H. S. Jung, X. Chen, J. S. Kim, J. Yoon, *Chem. Soc. Rev.* **2013**, *42*, 6019-6031.
[14] L. Y. Niu, Y. Z. Chen, H. R. Zheng, L. Z. Wu, C. H. Tung, Q. Z. Yang, *Chem. Soc. Rev.* **2015**, *44*, 6143-6160.
[15] C. Yin, K.-M. Xiong, F. Huo, J. C. Salamanca, R. M. Strongin, *Angew. Chem.* **2017**, 129, 13368-13379; *Angew. Chem. Int. Ed.*, **2017**, *56*, 13188-13198.
[16] W. Chen, H. Luo, X. Liu, J. W. Foley, X. Song, *Anal. Chem.* **2016**, *88*, 3638-3646.
[17] Y. Kim, M. Choi, S. V. Mulay, M. Jang, J. Y. Kim, W.-H. Lee, S. Jon, D. G. Churchill, *Chem. Eur. J.* **2018**, *24*, 5623-5629.
[18] K. Wang, T. Leng, Y. Liu, C. Wang, P. Shi, Y. Shen, *Sens. Actuat. B-Chem.* **2017**, *248*, 338-345.
[19] L. Y. Niu, Y. S. Guan, Y. Z. Chen, L. Z. Wu, C. H. Tung, Q. Z. Yang, *J. Am. Chem. Soc.* **2012**, *134*, 18928-18931.
[20] M. Işık, R. Guliyev, S. Kolemen, Y. Altay, B. Senturk, T. Tekinay, E. U. Akkaya, *Org. Lett.* **2014**, *16*, 3260-3263.
[21] S. Y. Lim, K. H. Hong, D. I. Kim, H. Kwon, H. J. Kim, *J. Am. Chem. Soc.* **2014**, *136*, 7018-7025.
[22] J. Liu, Y. Q. Sun, Y. Huo, H. Zhang, L. Wang, P. Zhang, D. Song, Y. Shi, W. Guo, *J. Am. Chem. Soc.* **2014**, *136*, 574-577.
[23] X. Chen, Y. Wang, R. Chai, Y. Xu, H. Li, B. Liu, *ACS Appl. Mater. Interfaces* **2017**, *9*, 13554-13563.
[24] M. Cao, H. Chen, D. Chen, Z. Xu, S. H. Liu, X. Chen, J. Yin, *Chem. Commun.* **2016**, *52*, 721-724.
[25] H.-J. Xiang, H. P. Tham, M. D. Nguyen, S. Z. F. Phua, W. Q. Lim, J.-G. Liu, Y. Zhao, *Chem. Commun.* **2017**, *53*, 5220-5223.
[26] Z. Liu, X. Zhou, Y. Miao, Y. Hu, N. Kwon, X. Wu, J. Yoon, *Angew. Chem.* **2017**, 129, 5906-5910; *Angew. Chem. Int. Ed.* **2017**, *56*, 5812-5816.
[27] L. Chen, J.-S. Park, D. Wu, C.-H. Kim, J. Yoon, *Sensor. Actuat. B-Chem.* **2018**, *262*, 306-312.
[28] Y. Qi, Y. Huang, B. Li, F. Zeng, S. Wu, *Anal. Chem.* **2018**, *90*, 1014-1020.
[29] Z. Mao, M. Wang, J. Liu, L.-J. Liu, S. M.-Y. Lee, C.-H. Leung, D.-L. Ma, *Chem. Commun.* **2016**, *52*, 4450-4453.
[30] Z.-H. Fu, X. Han, Y. Shao, J. Fang, Z.-H. Zhang, Y.-W. Wang, Y. Peng, *Anal. Chem.* **2017**, *89*, 1937-1944.
[31] Y. Yue, F. Huo, P. Ning, Y. Zhang, J. Chao, X. Meng, C. Yin, *J. Am. Chem. Soc.* **2017**, *139*, 3181-3185.
[32] L. Y. Niu, Y. S. Guan, Y. Z. Chen, L. Z. Wu, C. H. Tung, Q. Z. Yang, *Chem. Commun.* **2013**, *49*, 1294-1296.
[33] L. Song, T. Jia, W. Lu, N. Jia, W. Zhang, J. Qian, *Org. Biomol. Chem.* **2014**, *12*, 8422-8427.
[34] Y.-S. Guan, L.-Y. Niu, Y.-Z. Chen, L.-Z. Wu, C.-H. Tung, Q.-Z. Yang, *RSC Adv.* **2014**, *4*, 8360-8364.
[35] F. Wang, Z. Guo, X. Li, X. Li, C. Zhao, *Chem. Eur. J.* **2014**, *20*, 11471-11478.
[36] L. Ma, J. Qian, H. Tian, M. Lan, W. Zhang, *Analyst* **2012**, *137*, 5046-5050.
[37] Y. Liu, S. Zhang, X. Lv, Y. Q. Sun, J. Liu, W. Guo, *Analyst* **2014**, *139*, 4081-4087.
[38] H. Sunahara, Y. Urano, H. Kojima, T. Nagano, *J. Am. Chem. Soc.* **2007**, *129*, 5597-5604.
[39] F. Wang, J. An, L. Zhang, C. Zhao, *RSC Adv.* **2014**, *4*, 53437-53441.
[40] Y. Liu, X. Lv, M. Hou, Y. Shi, W.Guo, *Anal. Chem.* **2015**, *87*, 11475-11483.
[41] X. Shao, R. Kang, Y. Zhang, Z. Huang, F. Peng, J. Zhang, Y. Wang, F. Pan, W. Zhang, W. Zhao, *Anal. Chem.* **2015**, *87*, 399-405.
[42] X. Lu, W. Wang, Q. Dong, X. Bao, X. Lin, W. Zhang, X. Dong, W. Zhao, *Chem. Commun.* **2015**, *51*, 1498-1501.
[43] Y. Zhang, X. Shao, Y. Wang, F. Pan, R. Kang, F. Peng, Z. Huang, W. Zhang, W. Zhao, *Chem. Commun.* **2015**, *51*, 4245-4248.
[44] J. Zhang, J. Zhou, X. Dong, X. Zheng, W. Zhao, *RSC Adv.* **2016**, *6*, 51304-51309.
[45] J. Zhang, X. Bao, J. Zhou, F. Peng, H. Ren, X. Dong, W. Zhao, *Biosens. Bioelectron.* **2016**, *85*, 164-170.
[46] J. Zhang, X. Ji, J. Zhou, Z. Chen, X. Dong, W. Zhao, *Sensor. Actuat. B-Chem.* **2018**, *257*, 1076-1082.
[47] J. Zhang, X. Ji, H. Ren, J. Zhou, Z. Chen, X. Dong, W. Zhao, *Sensor. Actuat. B-Chem.* **2018**, *260*, 861-869.
[48] J. Gao, Y. Tao, N. Wang, J. He, J. Zhang, W. Zhao, *Spectrochim. Acta, Part A* **2018**, *203*, 77-84.
[49] N. Wang, M. Chen, J. Gao, X. Ji, J. He, J. Zhang, W. Zhao, *Talanta* **2019**, *195*, 281-289.
[50] N. Boens, V. Leen, W. Dehaen, *Chem. Soc. Rev.* **2012**, *41*, 1130-1172.
[51] T. Kowada, H. Maeda, K. Kikuchi, *Chem. Soc. Rev.* **2015**, *44*, 4953-4972.
[52] J. Liu, Y. Q. Sun, H. Zhang, Y. Huo, Y. Shi, W. Guo, *Chem. Sci.* **2014**, *5*, 3183-3188.
[53] D. H. Ma, D. Kim, E. Seo, S. J. Lee, K. H. Ahn, *Analyst* **2015**, *140*, 422-427.
[54] F. Wang, L. Zhou, C. Zhao, R. Wang, Q. Fei, S. Luo, Z. Guo, H. Tian, W.-H. Zhu, *Chem. Sci.* **2015**, *6*, 2584-2589.
[55] H. Kang, Y. Si, Y. Liu, X. Zhang, W. Zhang, Y. Zhao, B. Yang, Y. Liu, Z. Liu, *J. Phys. Chem. A* **2018**, 122, 5574-5579.
[56] A. Kamkaew, S. H. Lim, H. B. Lee, L. V. Kiew, L. Y. Chung, K. Burgess, *Chem. Soc. Rev.* **2013**, 42, 77-88.
[57] M. B. Halle, T. Yudhistira, W.-H. Lee, S. V. Mulay, D. G. Churchill, *Org. Lett.* **2018**, *20*, 3557-3561.
[58] T. Yudhistira S. V. Mulay, K. J. Lee, Y. Kim, H.-S. Park, D. G. Churchill, *Chem. Asian J.* **2017**, *12*, 1927-1934.
[59] A. P. Singh, K. M. Lee, D. P. Murale, T. Jun, H. Liew, Y.-H. Suh, D. G. Churchill, *Chem. Commun.* **2012**, *48*, 7298-7300.
[60] D. E. Ramírez-Ornelas, R. Sola-Llano, J. Bañuelos, I. L. Arbeloa, J. A. Martínez-Alvarez, H.r M. Mora-Montes, B. Franco, E. Peña-Cabrera, *ACS Omega* **2018**, *3*, 7783-7797.
[61] A. J. Gómez-Infante, J. Bañuelos, I. Valois-Escamilla, D. Cruz-Cruz, R. Prieto-Montero, I. López-Arbeloa, T. Arbeloa, E. Peña-Cabrera, *Eur. J. Org. Chem.* **2016**, 5009-5023.
[62] L. Betancourt-Mendiola, I. Valois-Escamilla, T. Arbeloa, J. Bañuelos, I. L. Arbeloa, J. Flores-Rizo, R. Hu, E. Lager, C. F. A. Gomez-Duran, J. L. Belmonte-Vazquez, M. R. Martínez-Gonzalez, I. J. Arroyo, C. A. Osorio-Martínez, E. Alvarado-Martínez, A. Urías-Benavides, B. D. Gutierrez-Ramos, B. Z. Tang, E. Peña-Cabrera, *J. Org. Chem.* **2015**, *80*, 5771-5782.
[63] H. Zhu, J. Fan, Q. Xu, H. Li, J. Wang, P. Gao and X. Peng, *Chem. Commun.* **2012**, *48*, 11766–11768.
[64] P. S. Becker, C. M. Cohen, S. E. Lux, *J. Biol. Chem.* **1986**, *261*, 4620-4628.
[65] M. Monici, Biotechnol. *Annu. Rev.* **2005**, *11*, 227-256.
[66] V. Ntziachristos, *Annu. Rev. Biomed. Eng.* **2006**, *8*, 1-33.
[67] V. J. Pansare, S. Hejazi, W. J. Faenza, R. K. Prud'homme, *Chem. Mater.* **2012**, *24*, 812-827.

[68] J. Chen, A. Burghart, A. Derecskei-Kovacs, K. Burgess, *J. Org. Chem.* **2000**, *65*, 2900-2906.
[69] H. X. Zhang, J. B. Chen, X. F. Guo, H. Wang, H. S. Zhang, *Anal. Chem.* **2014**, *86*, 3115-3123.
[70] V. Leen, P. Yuan, L. Wang, N. Boens, W. Dehaen, *Org. Lett.* **2012**, *14*, 6150-6153.
[71] Z. Chen, B. Lu, Z. Ding, K. Gao, N. Yoshikai, *Org. Lett.* **2013**, *15*, 1966-1969.
[72] W. W. Tan, X. Hou, N. Yoshikai, *Synthesis* **2014**, *46*, 2727-2733.

10.1002/chem.201902301

Layout 1:

FULL PAPER

In this work, we investigate the impact of substituents on 1,7 positions of the *meso*-arylmercapto BODIPY to biothiols. DM-BDP-SAr turned out to be a preferred probe for Cys with faster reaction rate. We further modified the probe with lysosomal targeting morpholine moiety and developed Lyso-S and Lyso-D as selective probes for Cys detection in lysosome.

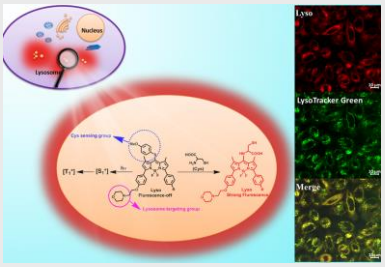

Jinhua Gao,[a] Yuanfang Tao,[a] Jian Zhang,[a] Nannan Wang,[a] Xin Ji,[a] Jinling He,[a] Yubing Si,*[c] and Weili Zhao*[ab]*

Page No. – Page No.

Development of lysosome-targeted fluorescent probes for Cys by regulating BODIPY molecular structure